Long-range *Pitx2c* enhancer–promoter interactions prevent predisposition to atrial fibrillation

Min Zhang[a,1], Matthew C. Hill[b,1], Zachary A. Kadow[b], Ji Ho Suh[c,d], Nathan R. Tucker[e,f], Amelia W. Hall[e,f], Tien T. Tran[g], Paul S. Swinton[g,h], John P. Leach[g], Kenneth B. Margulies[i], Patrick T. Ellinor[e,f], Na Li[c,d], and James F. Martin[b,d,g,h,2]

[a]Shanghai Children's Medical Center, Shanghai Jiao Tong University School of Medicine, 200127 Shanghai, China; [b]Program in Developmental Biology, Baylor College of Medicine, Houston, TX 77030; [c]Section of Cardiovascular Research, Department of Medicine, Baylor College of Medicine, Houston, TX 77030; [d]Cardiovascular Research Institute, Baylor College of Medicine, Houston, TX 77030; [e]Cardiovascular Research Center, Massachusetts General Hospital, Boston, MA 02129; [f]Program in Medical and Population Genetics, The Broad Institute of MIT and Harvard, Cambridge, MA 02142; [g]Department of Molecular Physiology and Biophysics, Baylor College of Medicine, Houston, TX 77030; [h]Texas Heart Institute, Houston, TX 77030; and [i]Penn Cardiovascular Institute, University of Pennsylvania Perelman School of Medicine, Philadelphia, PA 19104

Edited by Dan Roden, Vanderbilt University Medical Center, Nashville, TN, and accepted by Editorial Board Member Christine E. Seidman September 20, 2019 (received for review April 30, 2019)

Genome-wide association studies found that increased risk for atrial fibrillation (AF), the most common human heart arrhythmia, is associated with noncoding sequence variants located in proximity to *PITX2*. Cardiomyocyte-specific epigenomic and comparative genomics uncovered 2 AF-associated enhancers neighboring *PITX2* with varying conservation in mice. Chromosome conformation capture experiments in mice revealed that the *Pitx2c* promoter directly contacted the AF-associated enhancer regions. CRISPR/Cas9-mediated deletion of a 20-kb topologically engaged enhancer led to reduced *Pitx2c* transcription and AF predisposition. Allele-specific chromatin immunoprecipitation sequencing on hybrid heterozygous enhancer knockout mice revealed that long-range interaction of an AF-associated region with the *Pitx2c* promoter was required for maintenance of the *Pitx2c* promoter chromatin state. Long-range looping was mediated by CCCTC-binding factor (CTCF), since genetic disruption of the intronic CTCF-binding site caused reduced *Pitx2c* expression, AF predisposition, and diminished active chromatin marks on *Pitx2*. AF risk variants located at 4q25 reside in genomic regions possessing long-range transcriptional regulatory functions directed at *PITX2*.

atrial fibrillation | PITX2 | genome topology | epigenetics

Atrial fibrillation (AF) increases the risk of death, stroke, heart failure, and dementia. AF incidence increases with age, and with life expectancy rising, AF prevalence will increase over the next decade. AF treatments, including stroke prevention and rate and rhythm control, have limited efficacy with side effects (1). Catheter ablation of ectopic foci, for drug refractory AF, carries the risk of procedural complications and recurrence. Given the challenges in treating AF, it is critical to develop a deeper understanding of molecular pathways leading to AF.

Population-based genome-wide association studies (GWAS) identified many AF-associated loci (2–8). A recent meta-analysis of GWAS for AF identified over 100 AF risk loci (7). The region most significantly associated with AF in European, Japanese, and African American populations is located on chromosome 4q25 (7). The gene in closest proximity to these 4q25 variants is the paired-like homeodomain transcription factor 2 (*PITX2*). *PITX2* encodes a homeobox transcription factor that is required for mammalian development. There are 3 *PITX2* isoforms (*PITX2a*, *PITX2b*, and *PITX2c*), and the major cardiac isoform is *PITX2c*. Previous work carried out in mice indicated that *Pitx2* haploinsufficiency and conditional postnatal ablation promotes an atrial arrhythmogenic phenotype (9–11). Postnatally, *Pitx2* is expressed in the left atrium (LA) and pulmonary vein, and its expression level decreases with age commensurate with onset of AF susceptibility in humans (11). AF often arises from ectopic electrical activity originating from the pulmonary veins and the LA, and *Pitx2* suppresses a pacemaker gene expression signature (11, 12). However, a functional connection between the upstream AF-associated gene desert, *PITX2* expression, and predisposition to AF has not been shown.

Insight into how intergenic noncoding GWAS single-nucleotide polymorphisms (SNPs) contribute to disease risk remain a challenge (13). It is thought that noncoding variants reside within or near regulatory elements controlling expression of distal target genes through topological interactions. However, the chromatin state of regulatory elements is variable across individuals, and the disruption of single transcription factor binding sites may not have any measurable phenotypic effect (14). Modeling risk variants in animal models is further complicated by the differences in regulatory sequence composition that have accumulated over millions of years of evolution. Even deletion of the most "ultra-conserved" enhancers may not produce detectable phenotypes (15, 16).

Chromosome conformation capture (3C) discovered a topological connection between potential enhancers within the 4q25

Significance

Noncoding single-nucleotide polymorphisms (SNPs) associated with atrial fibrillation (AF) remain poorly understood. Significant AF-associated risk variants are located upstream of *PITX2*. No functional evidence directly links this noncoding region to *PITX2* expression and AF. We identified a murine *Pitx2* enhancer, the deletion of which results in AF predisposition providing insight into how noncoding variants at 4q25 promote AF.

Author contributions: M.Z., M.C.H., and J.F.M. designed research; M.Z., M.C.H., Z.A.K., J.H.S., T.T.T., P.S.S., and J.P.L. performed research; M.Z., M.C.H., N.R.T., K.B.M., and P.T.E. contributed new reagents/analytic tools; M.Z., M.C.H., A.W.H., and N.L. analyzed data; and M.Z., M.C.H., and J.F.M. wrote the paper.

Competing interest statement: P.T.E. is supported by a grant from Bayer AG to the Broad Institute focused on the genetics and therapeutics of cardiovascular disease and has consulted for Bayer AG, Novartis, and Quest Diagnostics. J.F.M. is a founder and owns shares in Yap Therapeutics.

This article is a PNAS Direct Submission. D.R. is a guest editor invited by the Editorial Board.

Data deposition: The left atrium Assay for Transposase Accessible Chromatin using Sequencing data presented in this article have been deposited in the Database of Genotypes and Phenotypes (accession no. phs001539.v1.p1). ATAC-sequencing postalignment bigwig format files are available on the Broad Institute's Cardiovascular Disease Knowledge Portal (http://broadcvdi.org/informational/data) and for direct download using gsutil from gs://cvdi_epigenome/Human/Left_Atrium/ and from gs://cvdi_epigenome/Human/Left_Ventricle/. All mouse sequencing data have been deposited in the Gene Expression Omnibus (accession no. GSE138530). All other relevant data supporting the findings made in this study are available within the paper, *SI Appendix*, and Datasets S1–S5, or from the corresponding author upon reasonable request.

[1]M.Z. and M.C.H. contributed equally to this work.

[2]To whom correspondence may be addressed. Email: jfmartin@bcm.edu.

This article contains supporting information online at www.pnas.org/lookup/suppl/doi:10.1073/pnas.1907418116/-/DCSupplemental.

First published October 21, 2019.

gene desert and the *Pitx2c* and *Enpep* promoters (17). Other studies on the most proximal association signal found an AF-associated SNP (rs2595104) that was correlated with altered *PITX2c* expression in human embryonic stem-cell–derived cardiomyocytes (CMs) (13). A Tbx5-binding site, located ∼150 kb upstream of *Pitx2*, had enhancer activity in vitro (18). However, the interaction between AF risk variants proximal to *PITX2* and the *PITX2c* promoter remains incompletely understood (19).

We generated a mouse model for studying the molecular and phenotypic features associated with 4q25 regulatory region disruption. Through LA CM-specific epigenomics, we determined the chromatin accessibility of the *PITX2* locus in humans and used these data to design CRISPR/Cas9 deletions in mice. We showed that deletion of a noncoding region upstream of *Pitx2* predisposes mice to AF. The disruption of the upstream *Pitx2* regulatory element led to a shift of chromatin marks on the *Pitx2* gene body. Analysis of mice with deletion of an intronic CCCTC-binding factor (CTCF) site in the *Pitx2* gene led to reduced *Pitx2* expression and AF predisposition. Our findings reveal direct functional topological interactions between *PITX2* and upstream genetic AF risk variants and provide insight into noncoding AF variants identified through GWAS.

Results

Epigenetic Characterization of Human LA Cardiomyocytes. Distal regulatory elements are placed into close proximity to the promoters they regulate via chromatin looping. We hypothesized that AF-associated SNPs, located at 4q25, may disrupt the transcription factor (TF) binding, enhancer activity, and enhancer–promoter looping responsible for maintaining physiologic levels of PITX2 (Fig. 1*A*). First, to investigate the epigenetic landscape specific to LA CMs, the most relevant cell type for AF, we performed Assay for Transposase Accessible Chromatin using Sequencing (ATAC-seq) (20) on PCM1-enriched nuclei (21) derived from frozen human LA and left ventricle (LV) tissue (Fig. 1*B*). We obtained CM-enriched ATAC-seq results from a total of 11 LA samples and 3 LV samples. Importantly, the LA CMs possessed high accessibility at known LA-specific loci, like *NPPA*, compared to LV CMs (Fig. 1*C*). Principal component analysis revealed that the LA samples clustered separately from LV samples (Fig. 1*D*). Differential accessibility analysis uncovered 4,962 LA-enriched peaks (Fig. 1*E* and Dataset S1). Of the annotated genes from these peaks, 219 overlapped with atrial-enriched human proteome (22) (Dataset S2). To look at differential TF activity between LA and LV CMs, we deployed the HINT-ATAC (Hmm-based IdeNtification of Transcription factor footprints for ATAC-seq) algorithm (23), which corrects for Tn5 transposase cleavage bias when searching for TF footprints (Fig. 1*F*). Among LA significant footprints, we identified the SP1-related motifs SHOX, ZNF740, and RREB1. Notably, RREB1 was also enriched in atrial proteomics analysis (22). LV CMs were enriched for JUN and FOS motifs, including the JDP2 (JUN Dimerization Protein 2) motif (Fig. 1*F*). De novo motif enrichment on LA-specific peaks combined with expression data on the same human tissue (7) uncovered similar TF motif enrichment, including SP1/4 (Fig. 1*G*).

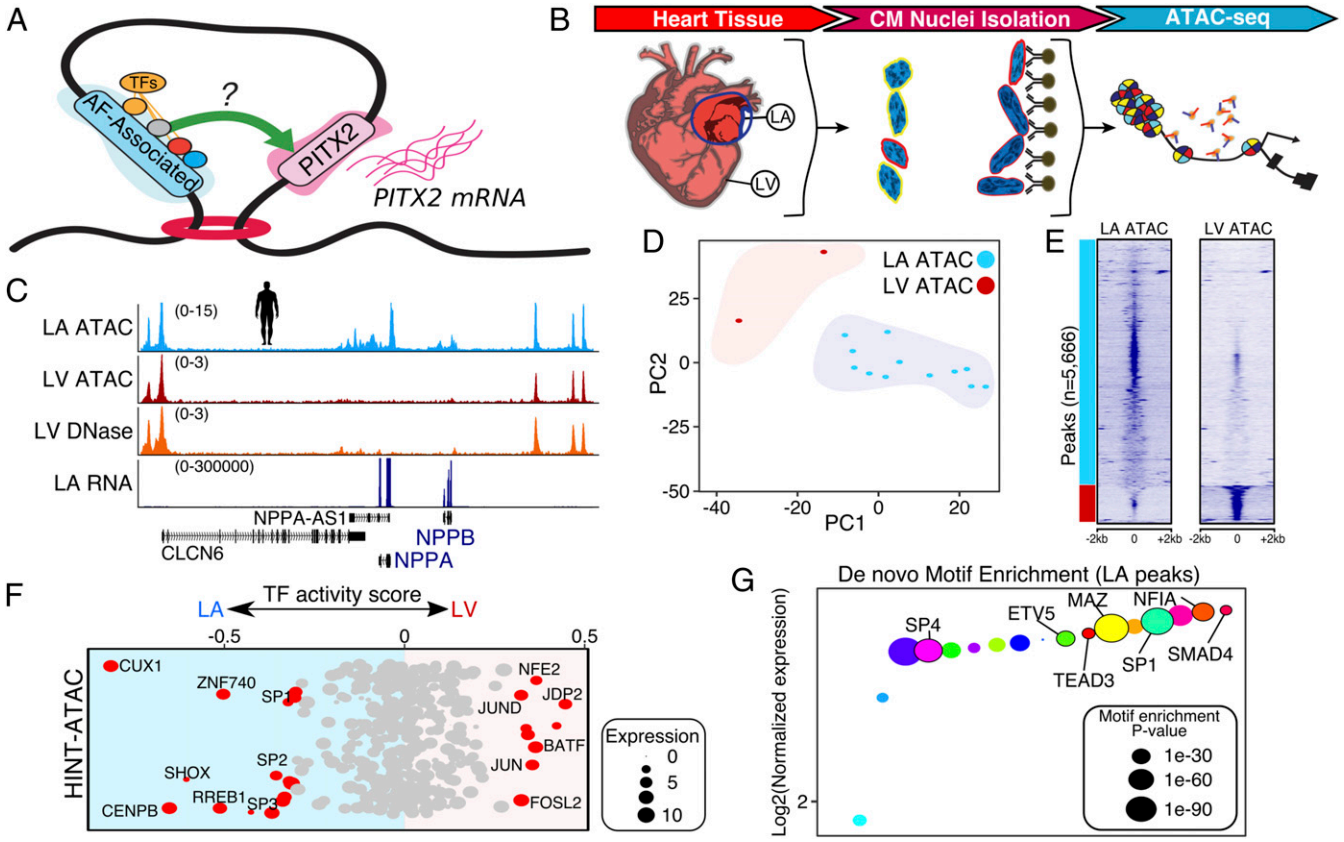

Fig. 1. LA human cardiomyocyte-specific ATAC-seq. (*A*) Graphical depiction of the putative topological association of the AF-associated region with *PITX2*. (*B*) Experimental strategy. (*C*) Genome browser track for *NPPA* and *NPPB*. (*D*) Principal component analysis of LA and LV ATAC-seq (adjusted *P* value < 0.01). (*E*) Heatmap of differentially accessible region-specific CM ATAC-seq peaks. (*F*) HINT-ATAC analysis of TF activity. Red TFs are those with absolute activity greater than 0.3. Dot size represents normalized expression. (*G*) De novo motif enrichment on LA enriched peaks (n = 4,962). TFs ranked by normalized LA expression. The size of each point indicates the motif enrichment *P* value.

A similar analysis using Cre-inducible Sun1-sfGFP INTACT mice (24) and CM-specific Cre recombinase (*Myh6*-MCM) to isolate LA, right atrium, and ventricular CM nuclei uncovered, by unsupervised clustering, a strong correlation between chromatin accessibility and active histone modifications on promoters and enhancers (*SI Appendix*, Fig. S1*A*). A total 3,205 LA-specific peaks were identified, including several annotated to LA markers *Nppa* and *Pitx2* (*SI Appendix*, Fig. S1 *B* and *C*).

AF-Associated Regions Located at 4q25 Possess Enhancer Characteristics. The human 4q25 gene desert, containing multiple regions that are independently associated with AF, is conserved in mice and encompasses ∼1 Mb on mouse chromosome 3. Within this 1-Mb region, genome organization is also conserved since *PITX2* and its neighboring genes are located in the same order and orientation in mice and humans. AF-associated regions are ∼150 kb upstream of *PITX2* (Fig. 2*A*). To investigate whether this region contained enhancers, we aligned this region against a multitissue human DNase Hypersensitivity (DHS) dataset (25). We found DHS peaks enriched in fetal human heart samples, but not in noncardiac tissue (Fig. 2*B*). These fetal heart DHS peaks aligned with our adult LA CM-specific ATAC peaks.

To investigate whether these peaks are potential enhancers, we aligned human LA CM ATAC-seq genomic tracks with human heart H3K4me1 chromatin immunoprecipitation sequencing (ChIP-seq), a marker of enhancer activity (26). ATAC peaks from LA aligned with the H3K4me1 peaks (Fig. 2*B*, boxed areas). ChromHMM, a machine-learning algorithm for characterizing chromatin states, predicted 2 cardiac enhancer blocks upstream of *PITX2C* (25). We narrowed down the 120-kb region into 2 blocks of 20 and 60 kb (Fig. 2*B*).

To identify the functional counterparts of these 2 putative enhancers in the mouse genome, we compared DNA sequence conservation (Fig. 2*C*). We identified 21 highly conserved DNA segments spread across these 2 blocks. Consistent with a previous report that cardiac enhancers are less conserved (27), we found only 1 of 3 human ATAC-seq peaks within the 60-kb block, and 2 of 4 in the 20-kb block contained highly conserved DNA sequences (Dataset S3). Nonetheless, we found the mouse counterpart of the 20-kb block contained 2 LA-enriched CM ATAC-seq peaks, while the 60-kb block was relatively inaccessible (Fig. 2*D*). These mouse LA-ATAC peaks were enriched for the active histone mark H3K27ac (27) (Fig. 2*D*). Motif enrichment using enhancers identified from both humans and mice revealed that consensus binding sites for Pitx2, Hnf4a, Nrf2, Ets, and Nkx factors were enriched (*SI Appendix*, Fig. S2), consistent with previous studies (28–30).

A Conserved 20-kb Enhancer Topologically Engages the *Pitx2c* Promoter. The *Pitx2* gene body is located on the boundary of 2 distinct topologically associated domains (TADs) (*SI Appendix*, Fig. S3). CTCF-mediated loop formation follows a simple rule, in which only a pair of distant CTCF-binding sites with convergent motif orientations form stable loops (31, 32). To determine TAD landscapes for the *PITX2* locus, we determined CTCF motif orientation of all CTCF ChIP-seq peaks (Fig. 3*A*). CTCF motif polarity was highly conserved between mice and humans (Fig. 3*B*).

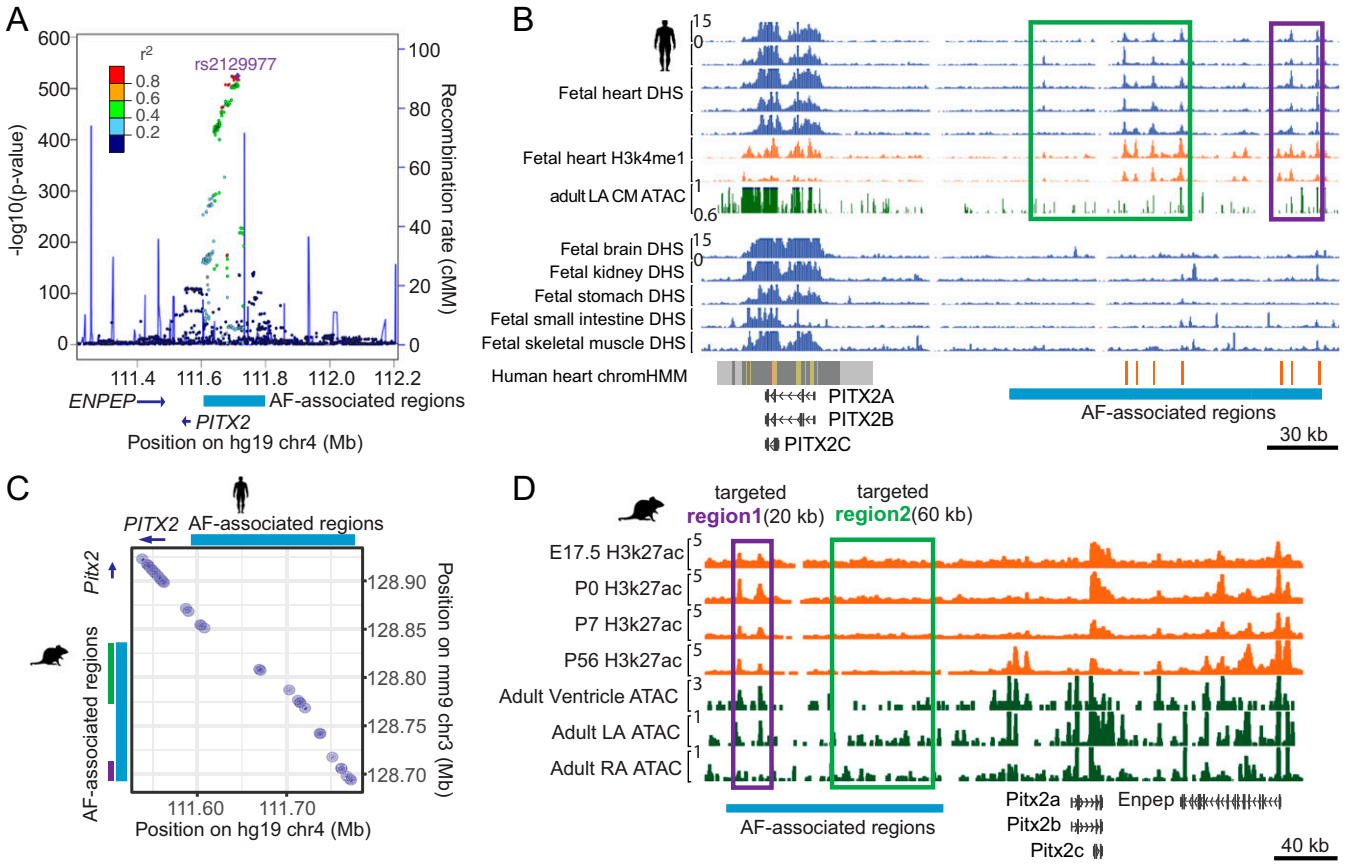

Fig. 2. Epigenomics guided interrogation of AF-associated 4q25 Locus. (*A*) Regional plot for PITX2 AF association. (*B*) Human LA-CM specific ATAC-seq and DHS (GSE18927), H3K4me1 ChIP-seq and chromatin HMM. Specific peaks indicated by orange bars on ChromHMM track. (*C*) Pitx2 human and mouse conservation. (*D*) Mouse genomic counterparts of AF-associated regions.

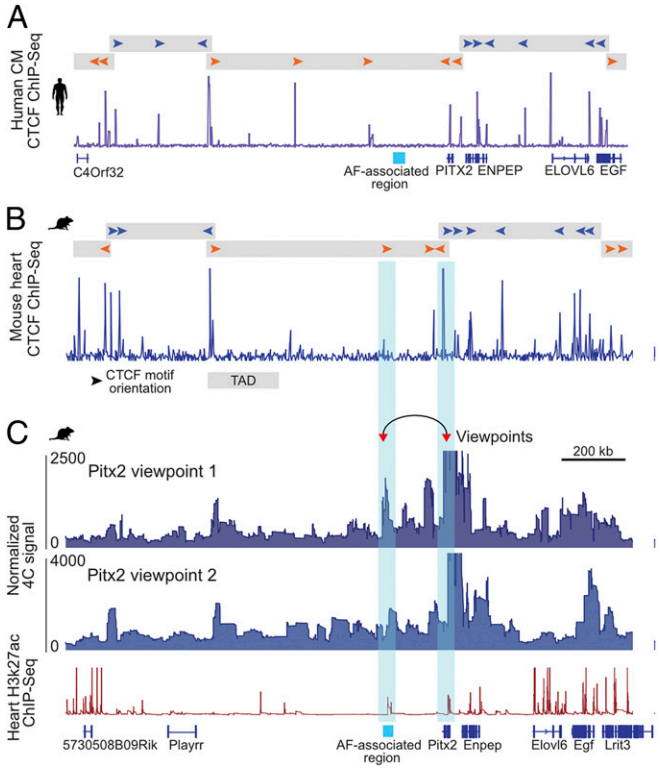

Fig. 3. *Pitx2c* topologically interacts with AF-associated enhancer in mouse heart. (*A*) CTCF-binding polarity. CTCF motif orientation (arrowheads). TAD organization highlighted (gray blocks). (*B*) CTCF-binding polarity in mouse heart. (*C*) 4C-seq across 2 *Pitx2* viewpoints (highlighted). AF-associated region and *Pitx2* gene body highlighted (cyan).

To obtain a higher-resolution view of enhancer–promoter interactome directed at *Pitx2c*, we performed chromosome conformation capture with high-throughput sequencing (4C-Seq) on postnatal day 8 mouse hearts using the *Pitx2c* promoter as the viewpoint. We found direct topological contacts between the 20-kb AF-associated enhancer and the *Pitx2c* promoter (Fig. 3*C*). Consistent with previous work, we also saw long-range *Pitx2c* promoter contacts with *Playrr*, a long non-coding RNA (33). The 4C-Seq revealed extensive contacts between *Pitx2c* and *Enpep*, as previously detected with 3C (Fig. 3*C* and *SI Appendix*, Fig. S4) (17). We also detected contacts between the *Pitx2c* promoter and a gene-dense region in the non–AF-associated TAD, containing genes like *Egf* and *Lrit3*. These data indicate that the topological architecture of the *Pitx2* locus in cardiac tissue is complex, and the presence of long-range contacts between the 20-kb AF-associated enhancer region and the *Pitx2c* promoter was evident.

Deletion of a Noncoding 20-kb AF-Associated Region Predisposes Mice to AF. To investigate how the AF-associated regulatory elements contribute to arrhythmogenesis, we used CRISPR/Cas9 editing to delete mouse counterparts of the aforementioned 20- and 60-kb enhancer blocks (Fig. 4 *A* and *B*). We obtained multiple homozygous mutant mouse lines for both the 20-kb deletion and the 60-kb deletion, which we refer to as $Pitx2^{\Delta E20k}$ and $Pitx2^{\Delta E60k}$ (Fig. 4 *C* and *D*). Both the $Pitx2^{\Delta E20k}$ and $Pitx2^{\Delta E60kb}$ mouse lines were viable and fertile.

We subjected mice to programmed intracardiac stimulation and found that $Pitx2^{\Delta E20k}$ mice were prone to AF (Fig. 5 *A*–*C*). In contrast, $Pitx2^{\Delta E60k}$ mice did not have a phenotype in either incidence of induced AF or length of AF burden (Fig. 5 *B* and *C*). Male $Pitx2^{\Delta E20k}$ mice were more prone to AF than females (Fig. 5*D*). To address if the deletion of the 20-kb enhancer alters *Pitx2*

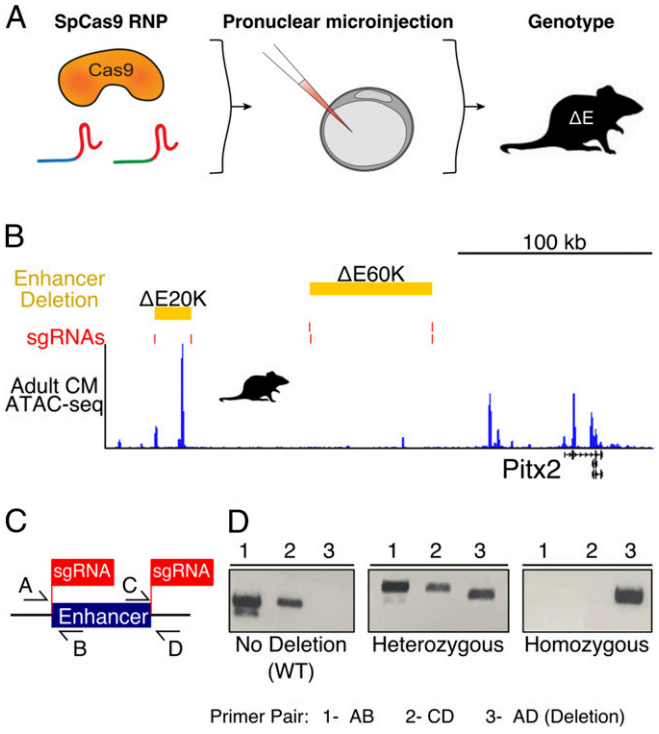

Fig. 4. Targeted genetic deletion of AF-associated regions. (*A*) Workflow for generation of enhancer deletions with CRISPR/Cas9 genomic editing. (*B*) Locations of deleted regions. (*C*) Genotyping strategy. (*D*) Representative genotyping from ΔE20K founders.

expression, we quantified LA *Pitx2c* expression via RNA-seq (Fig. 5*E*). In male homozygous $Pitx2^{\Delta E20k}$ mice, LA *Pitx2c* expression was reduced compared to controls, which we confirmed by quantitative RT-PCR (qRT-PCR) (*SI Appendix*, Fig. S4*A*). *Pitx2c* reduction was not observed in female mice (Fig. 5*E*). *Enpep* and

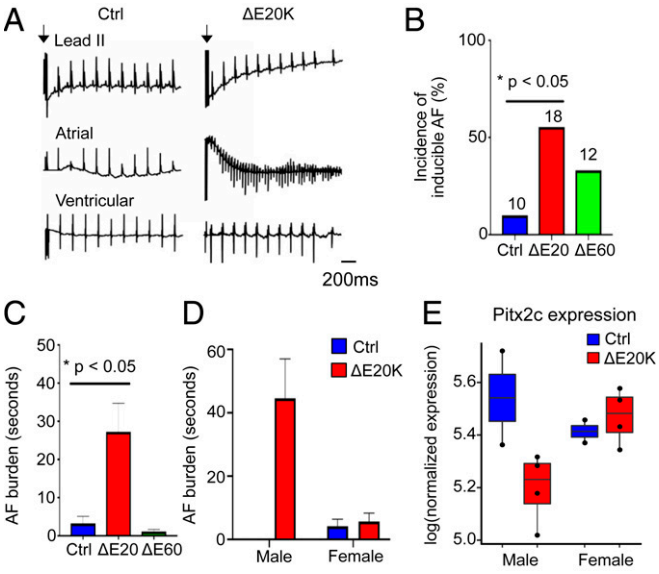

Fig. 5. Pitx2 enhancer deletion #1 (ΔE20K) AF susceptibility. (*A*) Representative recordings of surface ECG (Lead II), atrial electrogram, and ventricular electrogram where arrow indicates end of intracardiac pacing. (*B*) Incidence of intracardiac pacing induced AF. (*C*) AF burden, calculated as average length of AF following pacing. (*D*) AF burden by sex. (*E*) *Pitx2c* expression level in LA.

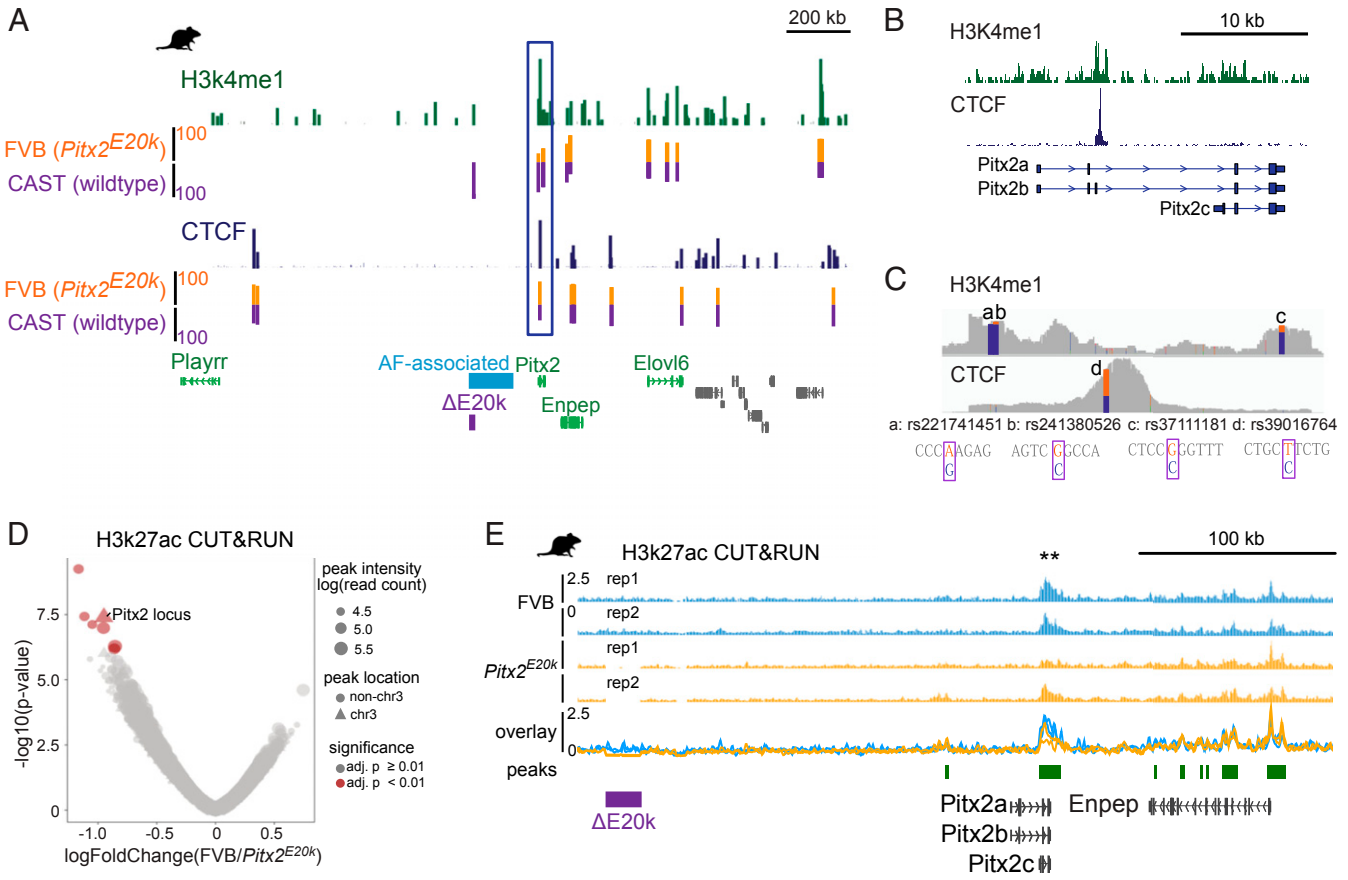

Fig. 6. AF-associated enhancer deletion alters local *Pitx2* chromatin landscape. (*A*) Allele-specific H3K4me1 and CTCF ChIP-Seq in FVB ΔE20K/CAST hybrids. Total mixed reads shown in green track. The expected odds for individual allelic SNP was 50% (orange bar for FVB background, purple bar for CAST). (*B*) A CTCF-binding peak, also enriched for H3K4me1 occupancy, located in the *Pitx2* intronic region. (*C*) Allele-specific H3K4me1 and CTCF-binding occupancy showing FVB (ΔE20K) strain-specific SNPs, rs221741451 (a), rs241380526 (b), and rs37111181 (c), rs39016764 (d). (*D*) CUT&RUN peak intensity of H3K27ac. (*E*) CUT&RUN of H3K27ac at Pitx2. $^{**}P < 0.01$.

Elovl6 were unchanged in male $Pitx2^{\Delta E20k}$ mice when compared to control males, but were elevated in female $Pitx2^{\Delta E20k}$ mice when compared to control females (*SI Appendix*, Fig. S4*B*). Differential expression analysis revealed that inflammation, cytoskeleton organization, and right atrial-identity genes, including *Bmp10*, were up-regulated in mutant LA tissue in both genders (*SI Appendix*, Fig. S4 *C–F*). Thus, the 20-kb AF-associated region encodes a *Pitx2c* enhancer that is required for the maintenance of *Pitx2c* expression in LA of adult male mice.

A Distal 20-kb Enhancer Is Required to Maintain *Pitx2* Gene Body Chromatin Status. Disruption of enhancer–promoter interactions can alter chromatin landscapes of topologically engaged regions (34). To determine whether the 20-kb enhancer acts as a functional *cis*-regulatory element for *Pitx2*, we crossed the $Pitx2^{\Delta E20k}$, FVB background, to the *Mus musculus castaneus* (Cast) subspecies to evaluate haplotype-specific chromatin landscapes (35). We performed H3K4me1 and CTCF ChIP-Seq on hearts from hybrid mice, extracted enriched peaks, and calculated haplotype-specific reads (Fig. 6 *A* and *B*). In the 20-kb enhancer region, H3K4me1 ChIP reads at the *Pitx2* gene body primarily originated from the control Cast allele (Fig. 6*C*). Interestingly, although we previously found direct contacts between the 20-kb enhancer region and several other distal gene promoters with 4C-seq, we did not observe such allelic H3K4me1 occupancy bias on other genes, such as *Enpep* or *Sec24*. Conversely, CTCF occupancy at both the *Pitx2* gene body and distal enhancer regions showed no significant differences between the 20-kb enhancer-deficient FVB allele and control Cast allele (Fig. 6*C*). We performed CUT&RUN on control (FVB) and homozygous $Pitx2^{\Delta E20k}$ to more quantitatively assess chromatin compositional shifts (36). The levels of active histone marks, including H3K27ac and H2K4me1, were significantly altered across the *Pitx2* gene body in $Pitx2^{\Delta E20k}$ mutants (Fig. 6 *D* and *E* and *SI Appendix*, Fig. S5 *A* and *B*). Conversely, CTCF and the inactive mark H3K27me3 were unchanged (*SI Appendix*, Fig. S5 *C–F*). These findings suggested that the 20-kb enhancer maintains the active chromatin state of *Pitx2* via long-range *cis*-interactions.

***Pitx2* Enhancer–Promoter Interactions Are Mediated by CTCF.** TAD boundaries are commonly CTCF-rich (37, 38). Given that *Pitx2* resides directly on a TAD boundary engaged by 2 distinct TADs, we wanted to dissect CTCF-dependent aspects of *Pitx2* gene regulation. A CTCF-binding site separates the 2 *Pitx2* promoters (*Pitx2ab* and *Pitx2c*). We hypothesized that this local CTCF site may play a bifunctional role in regulating both topological architecture and *Pitx2c* expression. Fortuitously, we had previously described a $Pitx2^{PZNeo}$ allele (ref. 39, designated δab^{hypoc}), in which the *Pitx2ab* isoform-specific exon 3 and part of the third intron, including the CTCF-binding site, were replaced with an internal ribosomal entry site-LacZ sequence (Fig. 7*A*).

qRT-PCR revealed that *Pitx2c* expression was reduced by about 50% in $Pitx2^{PZNeo/PZNeo}$ LA (Fig. 7*B*). Programmed stimulation on $Pitx2^{PZNeo/PZNeo}$ mice revealed that these mice were susceptible to

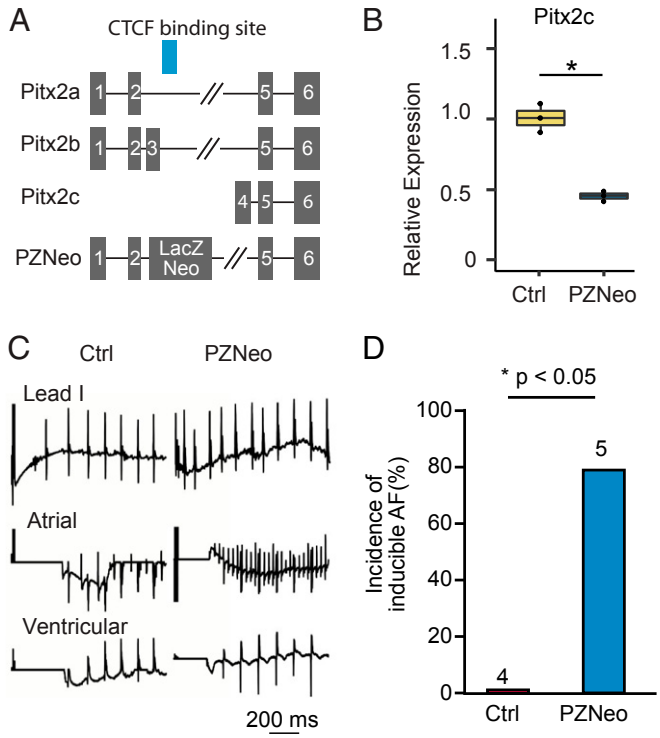

Fig. 7. CTCF-binding site deletion caused Pitx2 expression reduction and AF predisposition. (*A*) Illustration of *Pitx2*^{PZNeo} allele. (*B*) Quantitative PCR results from LA tissue of *Pitx2*$^{PZNeo/PZNeo}$ mice. (*C*) ECG tracing. (*D*) Incidence of intracardiac-pacing–induced AF.

atrial arrhythmias (Fig. 7 *C* and *D*). To determine the molecular consequences associated with a loss of local CTCF binding, we crossed *Pitx2*$^{PZNeo/PZNeo}$ with Cast mice and performed allele-specific CTCF ChIP-seq, as described above (*SI Appendix*, Fig. S6). CTCF occupancy on 4 of 30 CTCF sites increased in *Pitx2*^{PZNeo} compared to the Cast allele (*SI Appendix*, Fig. S6*A*). All 4 sites were located distal to *Pitx2*. Taken together, the genetic deletion of a CTCF-binding site located within the third intron of *Pitx2* caused a decrease in *Pitx2c* expression and an arrhythmogenic phenotype in mice.

Discussion

The connection between distal noncoding genetic variants and *PITX2* expression and AF predisposition has not been previously functionally verified. Using cell-type–specific epigenomics and comparative genomics, we identified 2 conserved putative enhancer elements that are associated with AF. Deletion of one of these regulatory elements in mice recapitulated the AF predisposition phenotype. This *Pitx2* regulatory element makes contact with *Pitx2c*, and the deletion of this element leads to dysregulation of the chromatin environment on the *Pitx2* gene body.

Pitx2 is expressed in multiple cell types at several developmental time points. During heart development *Pitx2c* is expressed in the LA, atrioventricular canal, cardiac outflow tract, right ventricle, left superior caval vein, and pulmonary vein myocardium (39, 40). Although it is surprising that homozygous ΔE20K and ΔE60K mice were phenotypically normal in the absence of physiologic stress, recent studies found that multiple enhancers with comparable activity proximal to the same gene are pervasive and function to confer phenotypic robustness (41). Previous work, looking at the 85-kb AF-associated region at 4q25, investigated human regulatory sequences in mouse cell lines and transgenic mice (*SI Appendix*, Fig. S7) (17). The authors concluded that these regulatory elements do not behave as cell-type–specific enhancers (17). It is likely that the activity of noncoding regulatory elements in mice and humans may have diverged. Indeed, as much as 30% of mammalian enhancers show evidence for functional gains and losses of TF-binding sites (42). Future work to dissect the regulatory elements driving tissue-specific *Pitx2* expression will make use of combinatorial pair-wise enhancer deletions.

We performed CM-enriched ATAC-seq on human LA tissue from "healthy" patients to prioritize the AF-associated risk variants found at 4q25. We did not observe a large overlap of AF risk variants with LA CM ATAC peaks most likely because the AF risk variants are markers of genomic locations, defined by linkage disequilibrium, rather than causative variants. If these nonaccessible sites do contain causative SNPs, then several possibilities exist to explain their function, including developmental activity, cell type and/or spatial specificity, and/or function during a response to some external stimulus or injury. Consistent with the presence of a stimulus response element, mouse models of neonatal cardiac injury have shown that *Pitx2* expression is induced by injury and is required for mitochondrial functional maintenance, the prevention of deleterious fat accumulation, and reactive oxygen species handling (30, 43). Alternatively, these unoccupied AF risk variants may initiate ectopic TF binding, which promotes deleterious gene expression patterns. Looking forward, the completion of large-scale cell-type–specific and tissue region resolved datasets in combination with high-throughput functional genomics experiments aimed at molecularly defining the roles of the 4q25 AF risk variants will help to resolve this important matter (44).

Materials and Methods

Detailed materials and methods provided in *SI Appendix*.

Mouse Alleles and CRISPR/Cas9-Mediated Deletion Lines. The Pitx2^{PZNeo} allele and INTACT mouse were described (24, 39).

Sequencing and Analysis. ChIP-seq was performed as described (30). ATAC-seq libraries were generated as described (20). The 4C protocol was followed as described (45). The 4C-seq data analysis pipeline was previously described (45).

Cardiomyocyte Nuclear Isolations. Nuclear isolation was done as described (24).

Programmed Intracardiac Pacing. Programmed intracardiac pacing was performed (11). Recordings of surface electrocardiogram (ECG) were done, and intracardiac electrograms were performed in anesthetized mice via right jugular vein catheterization.

Published Datasets Used in This Study. Human DHS-seq data was obtained from Gene Expression Omnibus (GEO) with entry GSE18927 (25). Mouse heart H3K27Ac ChIP-seq was extracted and reprocessed from GSE52386 (27).

ACKNOWLEDGMENTS. This work was supported by National Institutes of Health Grants DE023177, HL127717, HL130804, HL118761 (J.F.M.), F31HL136065 (M.C.H.), and HL140187 (N.R.T.); the Vivian L. Smith Foundation (J.F.M.); Fondation LeDucq Transatlantic Networks of Excellence in Cardiovascular Research Grant 14CVD01 (J.F.M., P.T.E.); Chinese Postdoctoral Science Foundation Grant 2016M601610 (M.Z.); Intellectual and Developmental Disabilities Research Center Grant 1U54 HD083092; the Eunice Kennedy Shriver National Institute of Child Health and Human Development; and Mouse Phenotyping Core Grant U54 HG006348.

1. N. J. Sethi *et al.*, The effects of rhythm control strategies versus rate control strategies for atrial fibrillation and atrial flutter: A systematic review with meta-analysis and trial sequential analysis. *PLoS One* **12**, e0186856 (2017).
2. E. J. Benjamin *et al.*, Variants in ZFHX3 are associated with atrial fibrillation in individuals of European ancestry. *Nat. Genet.* **41**, 879–881 (2009).
3. I. E. Christophersen *et al.*; METASTROKE Consortium of the ISGC; Neurology Working Group of the CHARGE Consortium; AFGen Consortium, Large-scale analyses of common and rare variants identify 12 new loci associated with atrial fibrillation. *Nat. Genet.* **49**, 946–952 (2017).
4. P. T. Ellinor *et al.*, Meta-analysis identifies six new susceptibility loci for atrial fibrillation. *Nat. Genet.* **44**, 670–675 (2012).

5. P. T. Ellinor *et al*., Common variants in KCNN3 are associated with lone atrial fibrillation. *Nat. Genet.* **42**, 240–244 (2010).
6. S. K. Low *et al*.; AFGen Consortium, Identification of six new genetic loci associated with atrial fibrillation in the Japanese population. *Nat. Genet.* **49**, 953–958 (2017).
7. C. Roselli *et al*., Multi-ethnic genome-wide association study for atrial fibrillation. *Nat. Genet.* **50**, 1225–1233 (2018).
8. M. F. Sinner *et al*.; METASTROKE Consortium; AFGen Consortium, Integrating genetic, transcriptional, and functional analyses to identify 5 novel genes for atrial fibrillation. *Circulation* **130**, 1225–1235 (2014).
9. P. Kirchhof *et al*., PITX2c is expressed in the adult left atrium, and reducing Pitx2c expression promotes atrial fibrillation inducibility and complex changes in gene expression. *Circ. Cardiovasc. Genet.* **4**, 123–133 (2011).
10. Y. Tao *et al*., Pitx2, an atrial fibrillation predisposition gene, directly regulates ion transport and intercalated disc genes. *Circ. Cardiovasc. Genet.* **7**, 23–32 (2014).
11. J. Wang *et al*., Pitx2 prevents susceptibility to atrial arrhythmias by inhibiting left-sided pacemaker specification. *Proc. Natl. Acad. Sci. U.S.A.* **107**, 9753–9758 (2010).
12. M. T. Mommersteeg *et al*., Pitx2c and Nkx2-5 are required for the formation and identity of the pulmonary myocardium. *Circ. Res.* **101**, 902–909 (2007).
13. J. Ye *et al*., A functional variant associated with atrial fibrillation regulates PITX2c expression through TFAP2a. *Am. J. Hum. Genet.* **99**, 1281–1291 (2016).
14. S. M. Waszak *et al*., Population variation and genetic control of modular chromatin architecture in humans. *Cell* **162**, 1039–1050 (2015).
15. N. Ahituv *et al*., Deletion of ultraconserved elements yields viable mice. *PLoS Biol.* **5**, e234 (2007).
16. D. E. Dickel *et al*., Ultraconserve enhancers are required for normal development. *Cell* **172**, 491–499.e15 (2018).
17. L. A. Aguirre *et al*., Long-range regulatory interactions at the 4q25 atrial fibrillation risk locus involve PITX2c and ENPEP. *BMC Biol.* **13**, 26 (2015).
18. R. D. Nadadur *et al*., Pitx2 modulates a Tbx5-dependent gene regulatory network to maintain atrial rhythm. *Sci. Transl. Med.* **8**, 354ra115 (2016).
19. F. Syeda, P. Kirchhof, L. Fabritz, PITX2-dependent gene regulation in atrial fibrillation and rhythm control. *J. Physiol.* **595**, 4019–4026 (2017).
20. J. D. Buenrostro, P. G. Giresi, L. C. Zaba, H. Y. Chang, W. J. Greenleaf, Transposition of native chromatin for fast and sensitive epigenomic profiling of open chromatin, DNA-binding proteins and nucleosome position. *Nat. Methods* **10**, 1213–1218 (2013).
21. R. Gilsbach *et al*., Dynamic DNA methylation orchestrates cardiomyocyte development, maturation and disease. *Nat. Commun.* **5**, 5288 (2014).
22. S. Doll *et al*., Region and cell-type resolved quantitative proteomic map of the human heart. *Nat. Commun.* **8**, 1469 (2017).
23. Z. Li *et al*., Identification of transcription factor binding sites using ATAC-seq. *Genome Biol.* **20**, 45 (2019).
24. A. Mo *et al*., Epigenomic signatures of neuronal diversity in the mammalian brain. *Neuron* **86**, 1369–1384 (2015).
25. A. Kundaje *et al*.; Roadmap Epigenomics Consortium, Integrative analysis of 111 reference human epigenomes. *Nature* **518**, 317–330 (2015).
26. F. Yue *et al*.; Mouse ENCODE Consortium, A comparative encyclopedia of DNA elements in the mouse genome. *Nature* **515**, 355–364 (2014).
27. A. S. Nord *et al*., Rapid and pervasive changes in genome-wide enhancer usage during mammalian development. *Cell* **155**, 1521–1531 (2013).
28. H. Shiratori *et al*., Two-step regulation of left-right asymmetric expression of Pitx2: Initiation by nodal signaling and maintenance by Nkx2. *Mol. Cell* **7**, 137–149 (2001).
29. H. Shiratori *et al*., Self-regulated left-right asymmetric expression of Pitx2c in the developing mouse limb. *Dev. Biol.* **395**, 331–341 (2014).
30. G. Tao *et al*., Pitx2 promotes heart repair by activating the antioxidant response after cardiac injury. *Nature* **534**, 119–123 (2016).
31. E. de Wit *et al*., CTCF binding polarity determines chromatin looping. *Mol. Cell* **60**, 676–684 (2015).
32. S. S. Rao *et al*., A 3D map of the human genome at kilobase resolution reveals principles of chromatin looping. *Cell* **159**, 1665–1680 (2014).
33. I. C. Welsh *et al*., Chromatin architecture of the Pitx2 locus requires CTCF- and Pitx2-dependent asymmetry that mirrors embryonic gut laterality. *Cell Rep.* **13**, 337–349 (2015).
34. K. Cao *et al*., SET1A/COMPASS and shadow enhancers in the regulation of homeotic gene expression. *Genes Dev.* **31**, 787–801 (2017).
35. A. Wutz, T. P. Rasmussen, R. Jaenisch, Chromosomal silencing and localization are mediated by different domains of Xist RNA. *Nat. Genet.* **30**, 167–174 (2002).
36. P. J. Skene, S. Henikoff, An efficient targeted nuclease strategy for high-resolution mapping of DNA binding sites. *eLife* **6**, 1–35 (2017).
37. E. P. Nora *et al*., Targeted degradation of CTCF decouples local insulation of chromosome domains from genomic compartmentalization. *Cell* **169**, 930–944.e22 (2017).
38. J. H. I. Haarhuis *et al*., The cohesin release factor WAPL restricts chromatin loop extension. *Cell* **169**, 693–707.e14 (2017).
39. C. Liu, W. Liu, M. F. Lu, N. A. Brown, J. F. Martin, Regulation of left-right asymmetry by thresholds of Pitx2c activity. *Development* **128**, 2039–2048 (2001).
40. D. Franco *et al*., Multiple transcriptional domains, with distinct left and right components, in the atrial chambers of the developing heart. *Circ. Res.* **87**, 984–991 (2000).
41. M. Osterwalder *et al*., Enhancer redundancy provides phenotypic robustness in mammalian development. *Nature* **554**, 239–243 (2018).
42. M. A. Flores, I. Ovcharenko, Enhancer reprogramming in mammalian genomes. *BMC Bioinf.* **19**, 316 (2018).
43. L. Li *et al*., *Pitx2* maintains mitochondrial function during regeneration to prevent myocardial fat deposition. *Development* **145**, pii: dev168609 (2018).
44. N. R. Tucker, S. Clauss, P. T. Ellinor, Common variation in atrial fibrillation: Navigating the path from genetic association to mechanism. *Cardiovasc. Res.* **109**, 493–501 (2016).
45. H. J. van de Werken *et al*., 4C technology: Protocols and data analysis. *Methods Enzymol.* **513**, 89–112 (2012).